

Supporting Information

Effect of the electron donating group on excited-state electronic nature and epsilon-near-zero properties of curcuminoid-borondifluoride dyes

Kyu-Ri Choi¹, Dae Hyeon Kim¹, Yeon Ui Lee², Virginie Placide¹, Steven Huynh¹, Dandan Yao³, Gabriel Canard³, Elena Zaborova³, Fabrice Mathevet^{4,7}, Loïc Mager,⁵ Benoît Heinrich⁵, Jean-Charles Ribierre⁶, Jeong Weon Wu,^{1*} Frédéric Fages,^{3*} Anthony D'Aléo^{3,5*}

¹ Department of Physics, Ewha Womans University, Seoul 03760, Republic of Korea

² Department of Physics, Chungbuk National University, Chungbuk 28644, Republic of Korea

³ Aix Marseille Univ, CNRS, CINaM UMR 7325, Campus de Luminy, Case 913, 13288 Marseille, France

⁴ Sorbonne Universités, Faculté des Sciences, CNRS, Parisien de Chimie Moléculaire (IPCM), UMR 8232, Chimie des Polymères, 75005 Paris, France

⁵ Université de Strasbourg, CNRS, Institut de Physique et Chimie des Matériaux de Strasbourg, UMR 7504, F-67000 Strasbourg, France

⁶ Center for Organic Photonics and Electronics Research (OPERA), Kyushu University, Fukuoka 819-0395, Japan

Contents

1. Table of spectroscopic data and photophysical properties
2. Cyclic voltammetry data
3. Squaraine solvatochromism
4. Grazing incidence wide angle x-ray scattering (GIWAXS)
5. Spectroscopic ellipsometry measurement
6. Reflection, transmission, absorption measurements and FDTD data

1. Table of spectroscopic data and photophysical properties

Absorption spectra was measured on Hitachi spectrophotometer U-3900, a double beam single monochromator system. Fluorescence spectra was measured on Horiba Jobin Yvon fluorimeter FluoroMax-4.

Table S1. Spectroscopic data and photophysical properties of compounds **1**, **2** and **3** in solvents of different polarity at room temperature^a

solvent	1			2			3		
	λ_{abs}	λ_{em}	$\Delta \nu_{ST}$	λ_{abs}	λ_{em}	$\Delta \nu_{ST}$	λ_{abs}	λ_{em}	$\Delta \nu_{ST}$
Cyclo	514	540	937	560	583	704	612	639	690
CCl ₄	522	558	1236	565	601	1060	626	665	937
Bu ₂ O	511	585	2475	564	614	1444	622	668	1107
Et ₂ O	506	607	3288	562	635	2046	624	673	1167
Chloroform	524	652	3747	593	698	2537	661	731	1449
BuOAc	507	642	4148	567	657	2416	631	690	1355
EtOAc	504	668	4871	568	677	2834	636	699	1417
DCM	516	709	5275	595	735	3201	665	749	1686
DCE	519	716	5301	594	732	3174	665	750	1704
Acetone	507	763	6618	580	730	3543	651	729	1644
ACN	507	805	7302	583	770	4166	661	756	1901

^a Absorption maximum wavelengths λ_{abs} (nm). Fluorescence maximum wavelengths λ_{em} (nm). Stokes shifts $\Delta \nu_{ST}$ (cm⁻¹). Cyclo: Cyclohexane. CCl₄: Carbon tetrachloride. Bu₂O: n-Dibutylether. Et₂O: Diethyl ether. BuOAc : n-Butylacetate. EtOAc: Ethyl acetate. DCM: Dichloromethane. DCE: 1,2-Dichloroethane. ACN: Acetonitrile.

Table S2. Spectroscopic data and photophysical properties of compounds **4**, **5** and **6** in solvents of different polarity at room temperature^a

solvent	4			5			6		
	λ_{abs}	λ_{em}	$\Delta \nu_{ST}$	λ_{abs}	λ_{em}	$\Delta \nu_{ST}$	λ_{abs}	λ_{em}	$\Delta \nu_{ST}$
Cyclo	562	575	402	594	606	333	620	637	430
CCl ₄	574	601	783	610	630	520	633	659	623
Bu ₂ O	574	602	810	608	640	901	636	666	708
Et ₂ O	576	616	1127	609	641	820	640	675	810
Chloroform	609	677	1649	643	684	932	682	729	945
BuOAc	586	641	1464	625	655	733	655	693	837
EtOAc	591	651	1559	625	661	871	660	701	886
DCM	620	698	1802	649	694	999	692	742	974
DCE	620	702	1884	651	696	993	695	744	948
Acetone	609	689	1907	641	683	959	681	726	910
ACN	618	713.5	2166	652	697	990	696	748	998

^a Absorption maximum wavelengths λ_{abs} (nm). Fluorescence maximum wavelengths λ_{em} (nm). Stokes shifts $\Delta \nu_{ST}$ (cm⁻¹). ; Cyclo: Cyclohexane. CCl₄: Carbon tetrachloride. Bu₂O: n-Dibutylether. Et₂O: Diethyl etherethylic ether. BuOAc : n-Butylacetate. EtOAcAcOEt: Eethyl acetate. DCM: Ddichloromethane. DCE: 1,2-Ddichloroethane. ACN: Aacetonitrile.

Table S3. Dielectric constant (ϵ), refractive index (n) and orientation polarizability ($\Delta f'$) of 11 solvents.

	Cyclohexane (Cyclo)	Carbon tetrachloride (CCl ₄)	n-Dibutylether (Bu ₂ O)	Diethyl ether (Et ₂ O)	Chloroform (CHCl ₃)	n-Butylacetate (BuOAc)
ϵ	2.02	2.24	3.1	4.33	4.81	5.07
n	1.426	1.416	1.399	1.352	1.443	1.392
$\Delta f'$	0.1,	0.118	0.196	0.251	0.251	0.269
	Ethylacetate (EtOAc)	Dichloromethane (DCM)	Dichloroethane (DCE)	Acetone	Acetonitrile (ACN)	
ϵ	6.02	8.93	10.5	20.7	37.5	
n	1.372	1.424	1.445	1.359	1.344	
$\Delta f'$	0.292	0.319	0.326	0.374	0.393	

2. Cyclic voltammetry data

Cyclic voltammetry (CV) data were acquired using a BAS 100 Potentiostat (Bioanalytical Systems) and a PC computer containing BAS100W software (v2.3). A three-electrode system with a Pt working electrode (diameter 1.6 mm), a Pt counter electrode and a Ag/AgCl (with a 3 M NaCl filling solution) reference electrode was used. $(n\text{-Bu})_4\text{NPF}_6$ (0.1 M in CH_2Cl_2) served as an inert electrolyte. Cyclic voltammograms were recorded at a scan rate of 100 mV s⁻¹ for solution of dyes at a concentration of *ca.* 10⁻³ M. Ferrocene was used as an internal standard

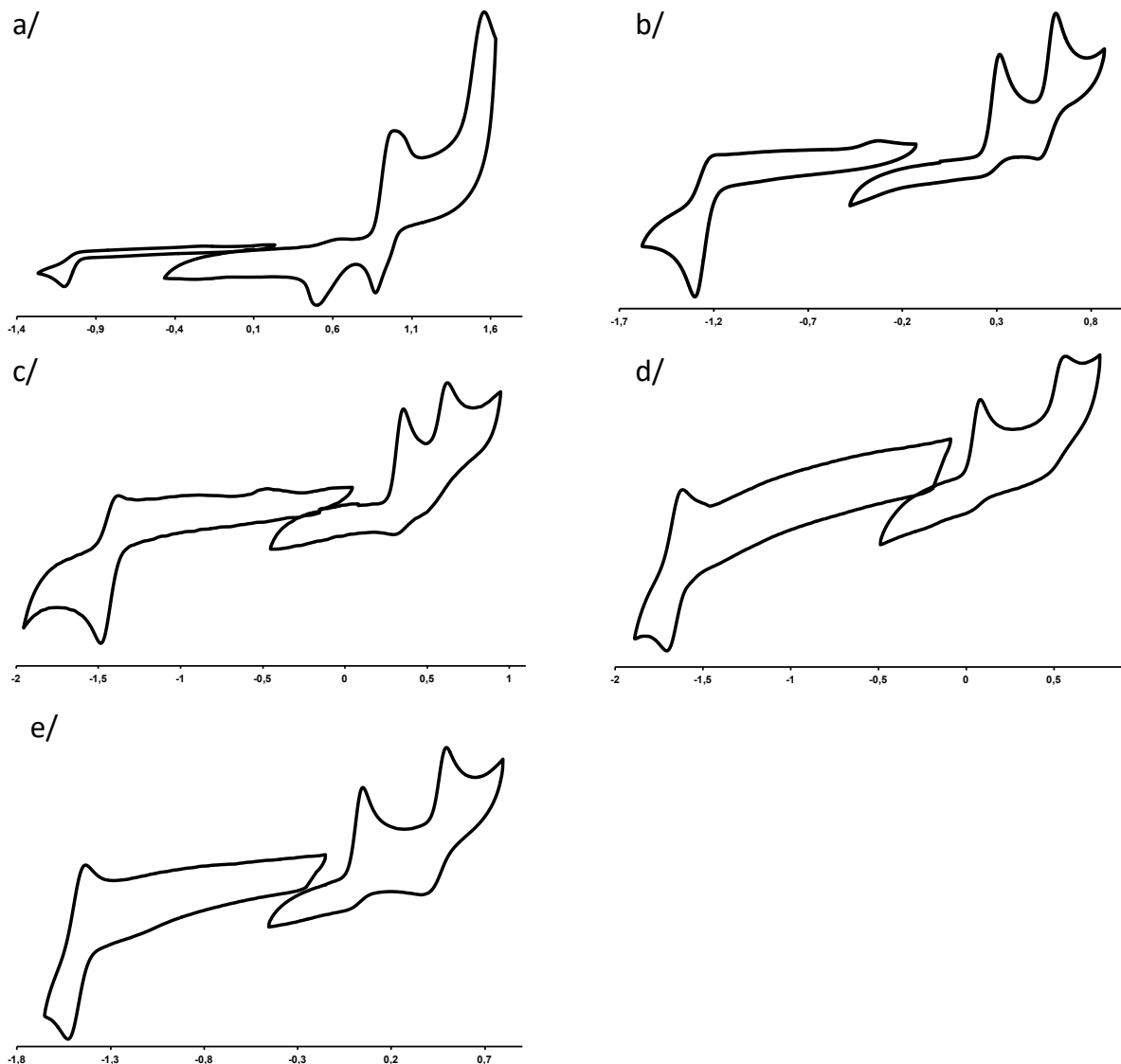


Figure S1| Cyclic voltammograms of **1** (a/), **3** (b/), **4** (c/), **5** (d/) and **6** (e/) in dichloromethane solution containing 0.1 M of $(n\text{-Bu})_4\text{NPF}_6$ (scan rate of 100 mV s⁻¹).

3. Solvatochromism of polymethine model squaraine

Molecular structure of polymethine model squaraine is shown in Figure S2, named as compound 7.

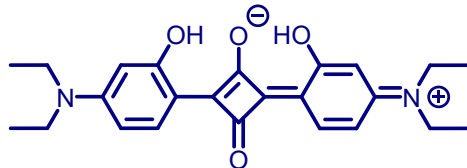


Figure S2| Molecular structure of polymethine model squaraine, compound 7.

Solvatochromism of compound 7 is shown in Figure S3.

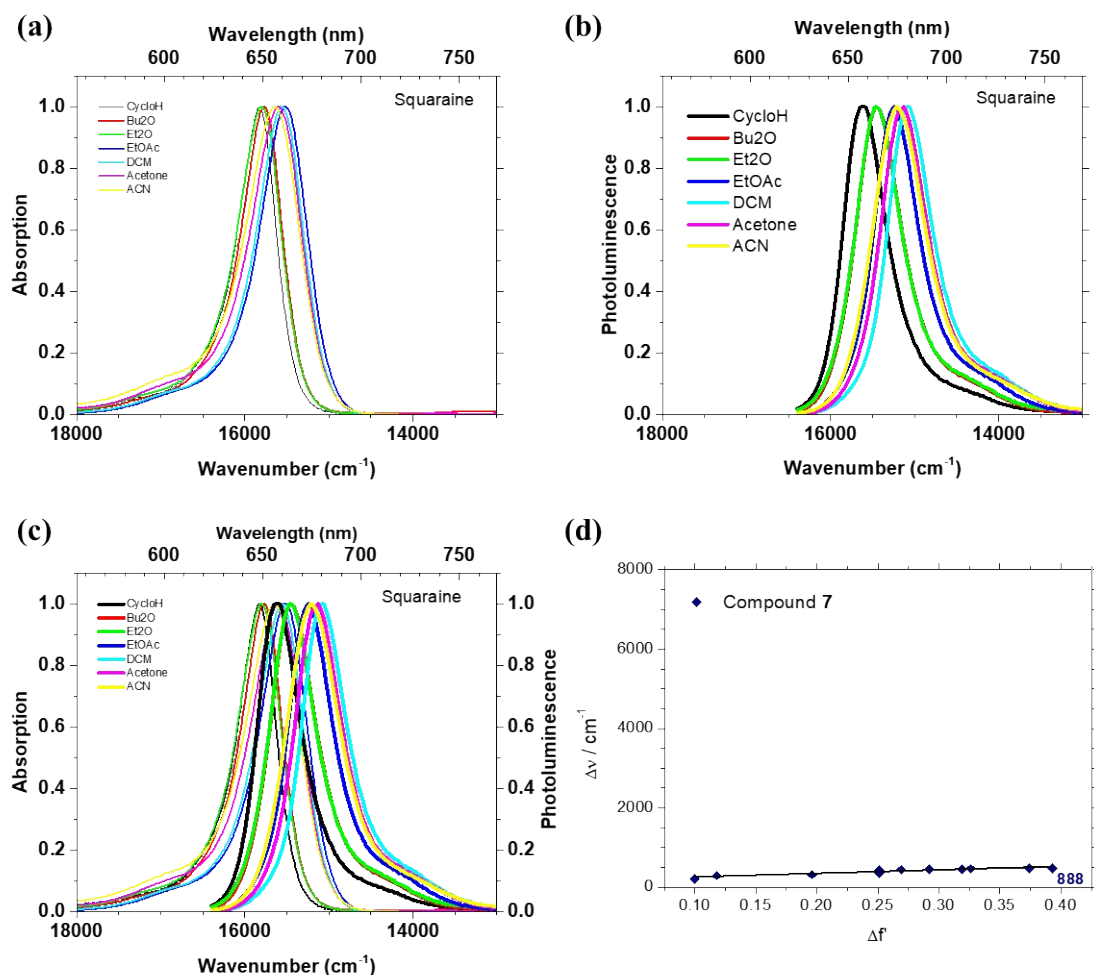


Figure S3| Solvatochromism of polymethine model squaraine 7. (a) and (b) show spectra of normalized absorption and normalized photoluminescence in 7 solvents with different polarity, namely, Cyclohexane (Cyclo), Bu_2O (dibutyl ether), Diethyl ether (Et_2O), Ethyl acetate (EtOAc), Dichloromethane (DCM), Acetone, Acetonitrile (ACN). (c) shows Stokes shift. (d) is the Lippert-Mataga plot of compound 7.

4. Grazing incidence wide angle x-ray scattering (GIWAXS)

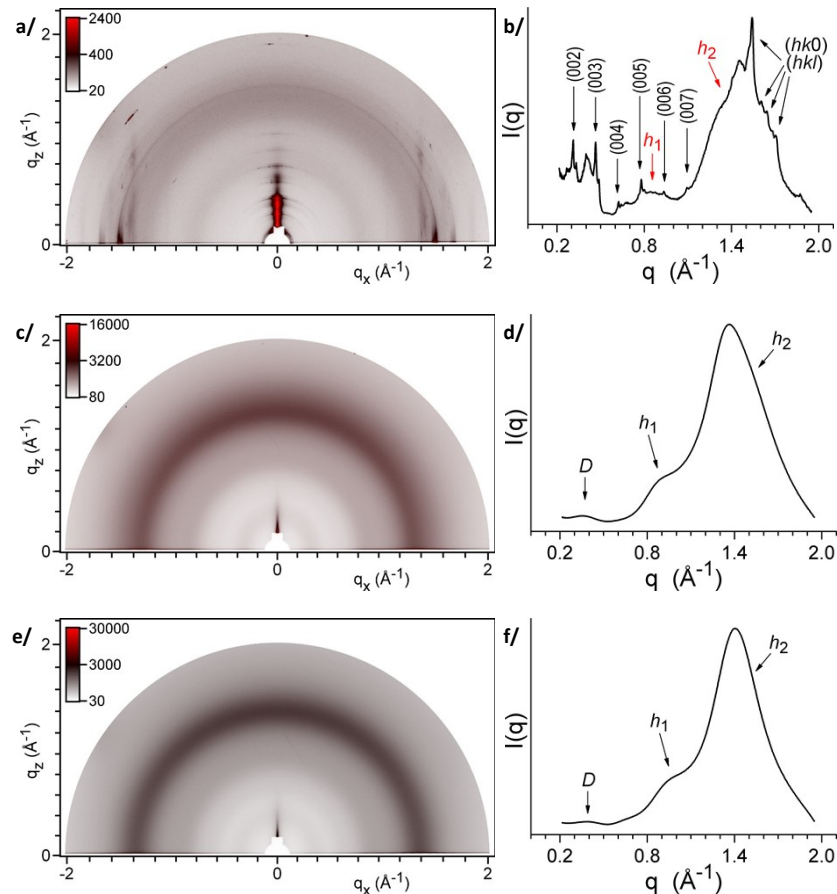


Figure S4| GIWAXS pattern (a/, c/ and e/) and the corresponding radial profile (b/, d/ and f/) of compound **1** (a/ and b/), **2** (c/ and d/) and **3** (e/ and f/).

The GIWAXS pattern (Fig S4 a/) and the corresponding radial profile (Fig S4 b/) of the pristine **1** film display coexistence of two phases: i) an amorphous phase (two broad scattering rings with maximums at $q = 0.8$ and 1.4 \AA^{-1} , for average lateral distances $h_1, h_2 = 2\pi/q = 7.8, 4.5 \text{ \AA}$) and ii) a lamellar crystalline phase (orders $(00l)$ of the lamellar periodicity $d = 40.5 \text{ \AA}$ and reflections $(hk0)$ and (hkl) of the in-plane arrangement and the three-dimensional structure). There is naturally no orientation of amorphous domains, while the crystalline domains adopt orientations with lamellae parallel to substrate.

The GIWAXS pattern (Fig S4 c/) and the corresponding radial profile (Fig S4 d/) of the pristine **2** film reveal an amorphous film, giving rise to broad rings from lateral distances between segments ($h_1, h_2 = 6.6, 4.5 \text{ \AA}$), and a broad small-angle ring from packing of entire molecules ($D = 17 \text{ \AA}$). The GIWAXS pattern (Fig S4 e/) and the corresponding radial profile (Fig S4 f/) of the pristine **3** film reveal an amorphous film, giving rise to broad rings from lateral distances between segments ($h_1, h_2 = 6.3, 4.5 \text{ \AA}$), and a broad small-angle ring from packing of entire molecules ($D = 17 \text{ \AA}$).

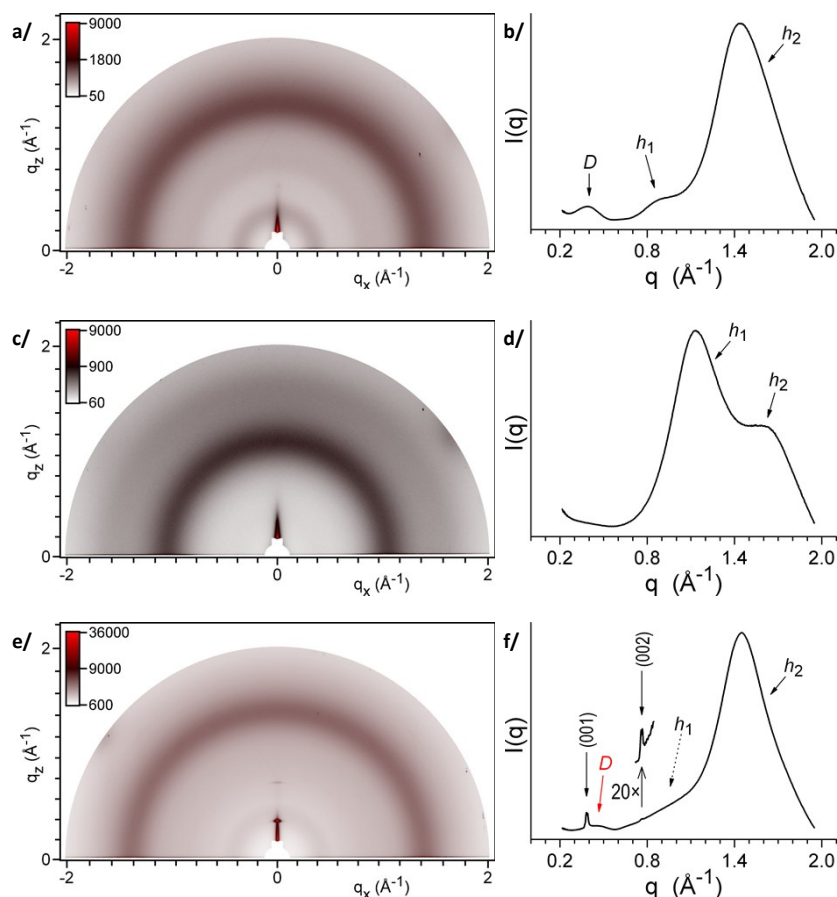


Figure S5| GIWAXS pattern (a/, c/ and e/) and the corresponding radial profile (b/, d/ and f/) of compound **4** (a/ and b/), **5** (c/ and d/) and **6** (e/ and f/).

The GIWAXS pattern (Fig S5 a/) and the corresponding radial profile (Fig S5 b/) of the pristine **4** film reveal an amorphous film, giving rise to broad rings from lateral distances between segments ($h_1, h_2 = 6.6, 4.3 \text{ \AA}$), and a broad small-angle ring from packing of entire molecules ($D = 16 \text{ \AA}$).

The GIWAXS pattern (Fig S5 c/) and the corresponding radial profile (Fig S5 d/) of the pristine **5** film reveal an amorphous film, giving rise to only two broad rings, with maximums at $q = 1.1$ and 1.6 \AA^{-1} ($h_1, h_2 = 5.6, 4.0 \text{ \AA}$) from lateral distances between molecular segments.

The GIWAXS pattern (Fig S5 e/) and the corresponding radial profile (Fig S5 f/) of the pristine **6** film display a smectic like structure with two sharp orders of a lamellar periodicity ($d = 16.3 \text{ \AA}$) generated by the alternation of aliphatic chain and aromatic core layers, besides broad rings from liquid-like lateral distances within layers ($h_2 = 4.3 \text{ \AA}$). The reflections align onto the meridian, which indicates that lamellae are oriented parallel to substrate. A continuous broad ring ($D = 14 \text{ \AA}$) moreover appears in the small-angle region, due to the liquid-like molecular packing within amorphous domains that coexist with the mesomorphic domains.

5. Spectroscopic ellipsometry measurement

The alpha SE spectroscopic ellipsometer was used at incident angle 70° to measure Ψ and Δ of the thin film from 380nm to 900nm. The rotating polarizer, photo-elastic modulator modulates between P-pol and S-pol from which the reflection ratio provides the information to unravel the dielectric index values of the thin films through Fresnel coefficient calculation. See Figure 5 for the dielectric permittivity spectra of all the six Curc series films. See Figures S6 for Ψ and Δ measurement and fitted data. See Figure S7 for the refractive index n and absorption coefficient k of all the six Curc series films. Model fitting parameters of the measured data are shown in Table S4 to 11. Each film is fitted from a substrate/transparent thin film/air model. Fitting is conducted through the sum of oscillator functions such as Gaussian and Tauc-Lorentz oscillators.

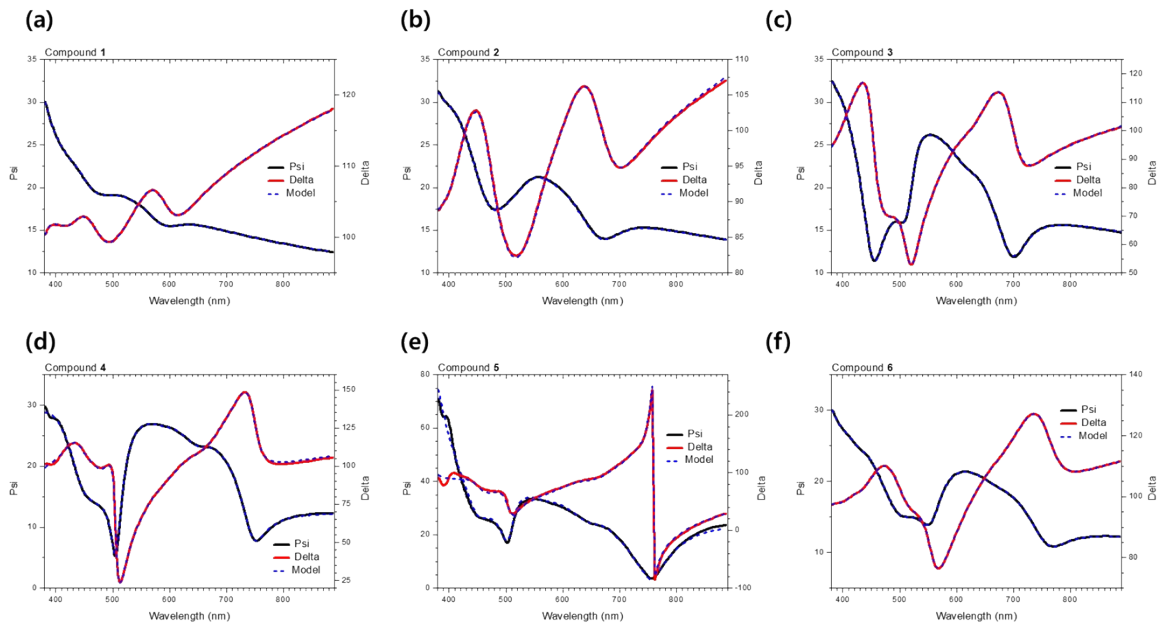


Figure S6| Measured Ψ , black, and Δ , red, spectroscopic ellipsometry data and fitted model, dashed blue of six Curc series films.

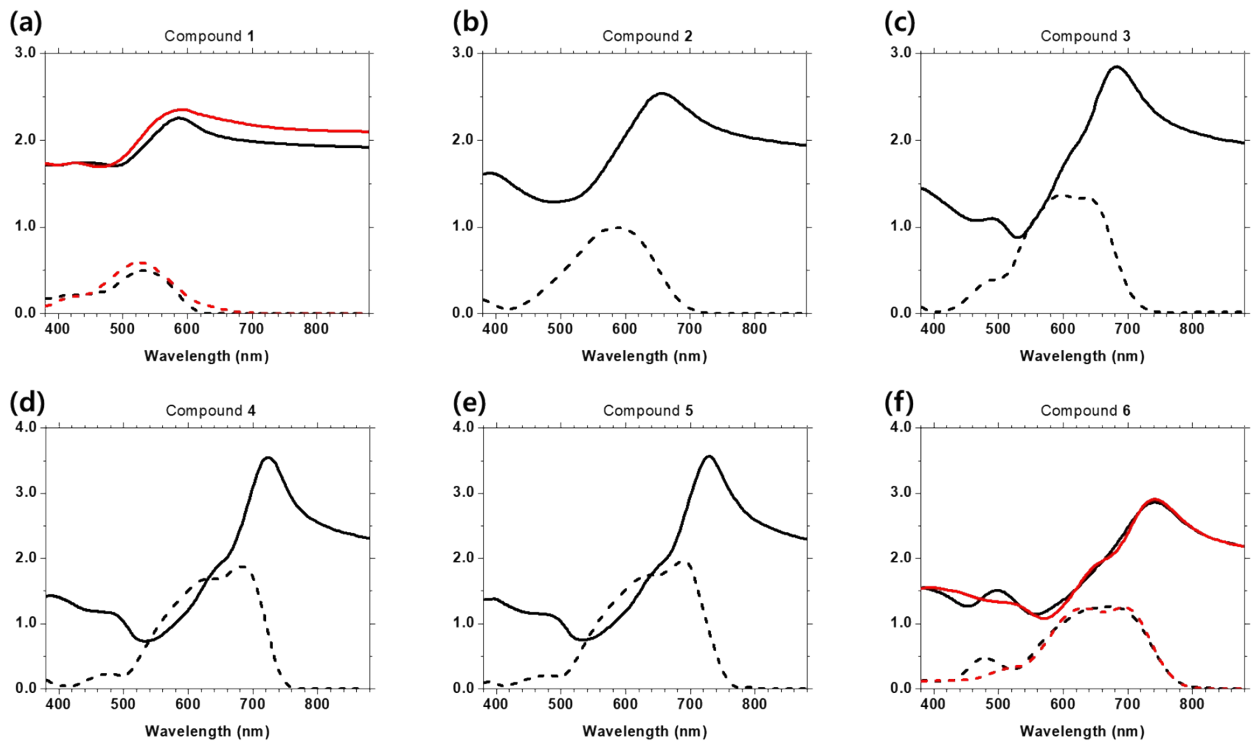


Figure S7| Refractive index n (solid curve) and absorption coefficient k (dashed curve) of all the six Curc series films are plotted. In (a) and (f) black and red curves correspond to ordinary and extra-ordinary components.

Table S4. Oscillator list for in-plane compound 1 dielectric permittivity

In-plane				
Number	Type	Amplitude	Broadening	Center energy
1	Gaussian	0.559	0.204	2.149
2	Gaussian	1.400	0.204	2.216
3	Gaussian	1.181	0.260	2.366
4	Gaussian	0.966	0.346	2.547
5	Gaussian	0.502	0.508	2.971
6	Gaussian	1.089	1.288	4.325

Table S5. Oscillator list for out-of-plane compound **1** dielectric permittivity

Out-of-plane				
Number	Type	Amplitude	Broadening	Center energy
1	Gaussian	0.523	0.208	2.150
2	Gaussian	1.421	0.195	2.193
3	Gaussian	1.258	0.257	2.361
4	Gaussian	0.975	0.330	2.531
5	Gaussian	0.572	0.608	2.923
6	Gaussian	0.550	0.576	3.823

Table S6. Oscillator list for compound **2** dielectric permittivity

Number	Type	Amplitude	Broadening	Center energy
1	Gaussian	2.410	0.206	1.957
2	Gaussian	2.539	0.268	2.102
3	Gaussian	1.268	0.323	2.269
4	Gaussian	0.798	0.409	2.508
5	Gaussian	0.569	0.499	3.338
6	Gaussian	0.076	0.228	2.806

Table S7. Oscillator list for compound **3** dielectric permittivity

Number	Type	Amplitude	Broadening	Center energy
1	Gaussian	4.043	0.152	1.873
2	Gaussian	4.632	0.274	2.028
3	Gaussian	1.187	0.208	2.241
4	Gaussian	0.655	0.339	2.488
5	Gaussian	0.435	0.377	3.444
6	Gaussian	0.268	0.417	2.662
7	Tauc-Lorentz	1.237	21.157	0.482

Table S8. Oscillator list for compound **4** dielectric permittivity

Number	Type	Amplitude	Broadening	Center energy
1	Gaussian	4.653	0.093	1.746
2	Gaussian	5.668	0.122	1.800
3	Gaussian	4.751	0.204	1.915
4	Gaussian	2.389	0.273	2.082
5	Gaussian	0.515	0.223	2.311
6	Gaussian	0.282	0.181	2.566
7	Gaussian	0.306	0.252	2.715
8	Gaussian	13.169	0.733	4.096
9	Tauc-Lorentz	32.099	0.088	1.690

Table S9. Oscillator list for compound **5** dielectric permittivity

Number	Type	Amplitude	Broadening	Center energy
1	Gaussian	4.670	0.093	1.726
2	Gaussian	6.101	0.123	1.787
3	Gaussian	5.068	0.243	1.911
4	Gaussian	1.718	0.339	2.125
5	Gaussian	0.338	0.259	2.626

Table S10. Oscillator list for in-plane compound **6** dielectric permittivity

In-plane				
Number	Type	Amplitude	Broadening	Center energy
1	Gaussian	1.316	0.122	1.695
2	Gaussian	2.590	0.157	1.756
3	Gaussian	3.467	0.260	1.859
4	Gaussian	2.089	0.353	2.066
5	Gaussian	1.150	0.323	2.570
6	Gaussian	0.413	2.034	3.589
7	Gaussian	47.977	0.025	0.024
9	Tauc-Lorentz	498.222	3.343	0.001

Table S11. Oscillator list for out-of-plane compound **6** dielectric permittivity

Out-of-plane				
Number	Type	Amplitude	Broadening	Center energy
1	Gaussian	2.408	0.146	1.715
2	Gaussian	3.008	0.160	1.755
3	Gaussian	3.023	0.218	1.894
4	Gaussian	2.175	0.277	2.027
5	Gaussian	0.653	0.371	2.335
6	Gaussian	0.365	0.460	2.587
7	Gaussian	0.071	0.173	2.867
8	Gaussian	0.390	0.567	3.158
9	Tauc-Lorentz	0.755	23.365	8.587

6. Reflection, transmission, absorption measurements and simulation data

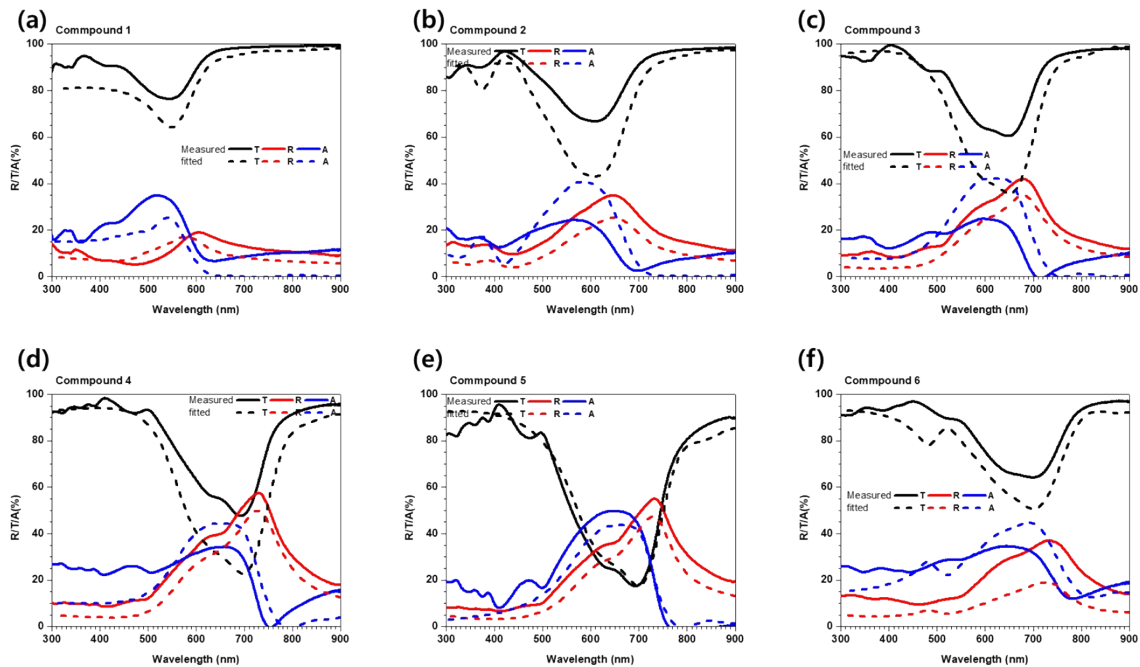


Figure S8| Measured data of six Curc series films (solid line) and simulated data (dashed line). Simulation data is obtained by use of dielectric permittivity spectrum of Figure 5.